Printed Circuit Heat Exchanger Steady-State Off-Design and Transient Performance Modeling in a Supercritical CO_2 Power Cycle

Vamshi Avadhanula and Timothy J. Held
Echogen Power Systems

ABSTRACT

This paper presents semi-empirical heat transfer and pressure-drop models of two large-scale Printed Circuit Heat Exchanger (PCHE) recuperator and heat rejection heat exchangers (HRHX) that were tested extensively on a 7.3MWe-scale sCO_2 power cycle. The models are discretized representations of the heat exchangers, which permits accommodation of the rapidly-varying thermodynamic and property variation of CO_2 over the pressure and temperature ranges encountered through the heat exchanger passages. The effects of assumed geometric details, such as passage dimensions, heat transfer enhancement, and internal cross-flow headers are modeled, and their impact on the predicted steady-state performance of the heat exchangers evaluated. Transient modeling of the heat exchangers also uses a discretized approach, including a discretized thermal mass model to predict the fluid outlet temperature evolution with time after rapid changes in inlet temperature, pressure and flow rate. For these cases, the inlet temperatures, pressures and flows are imposed based on measured values, and the outlet temperatures and pressures are modeled and compared to measurements.

INTRODUCTION

Supercritical carbon dioxide (sCO_2) power cycles are characterized by a high degree of recuperation, with the internally-recirculated heat frequently exceeding the rate of heat addition by a factor of three or more. The high conductance (UA) required for this large duty, accompanied by the high operating pressure of sCO_2 cycles requires the use of advanced, compact heat exchanger technology. The primary design used to date is the so-called "Printed Circuit Heat Exchanger" (PCHE), which consists of layers of chemically etched metal plates in a diffusion-bonded assembly [1]. These heat exchangers have proven to be robust in gas cooling service, with many years of successful field experience. While PCHEs have been proposed as the heat exchanger technology of choice for commercial-scale sCO_2 power cycles [2,3], practical experience for power-cycle applications has been limited to laboratory-scale systems [4–6] until recently, when a commercial-scale (7.3MWe) sCO_2 system, termed the EPS100, underwent an extensive factory test campaign [7].

Heat exchanger performance can be quantified in numerous ways. Heat transfer performance can be evaluated by conductance ($UA=Q/\Delta T_m$, where Q is the total transferred heat, and ΔT_m is an appropriately-defined mean temperature difference between the two fluid streams). The pressure drop across each side of the heat exchanger has an influence on both the heat transfer performance and overall cycle performance. Finally, heat exchanger life is critical to the successful deployment of sCO_2 power cycles. Heat exchanger life can be divided into performance degradation (e.g. fouling) and thermo-mechanical factors. Given that PCHEs are designed to ASME Boiler and Pressure Vessel code requirements, steady-state hydraulic and thermal stress are unlikely to be life-limiting. Thermomechanical life is more likely to be limited by severe thermal transients that could be generated during extreme incidents [8,9], such as emergency stops or turbine trips.

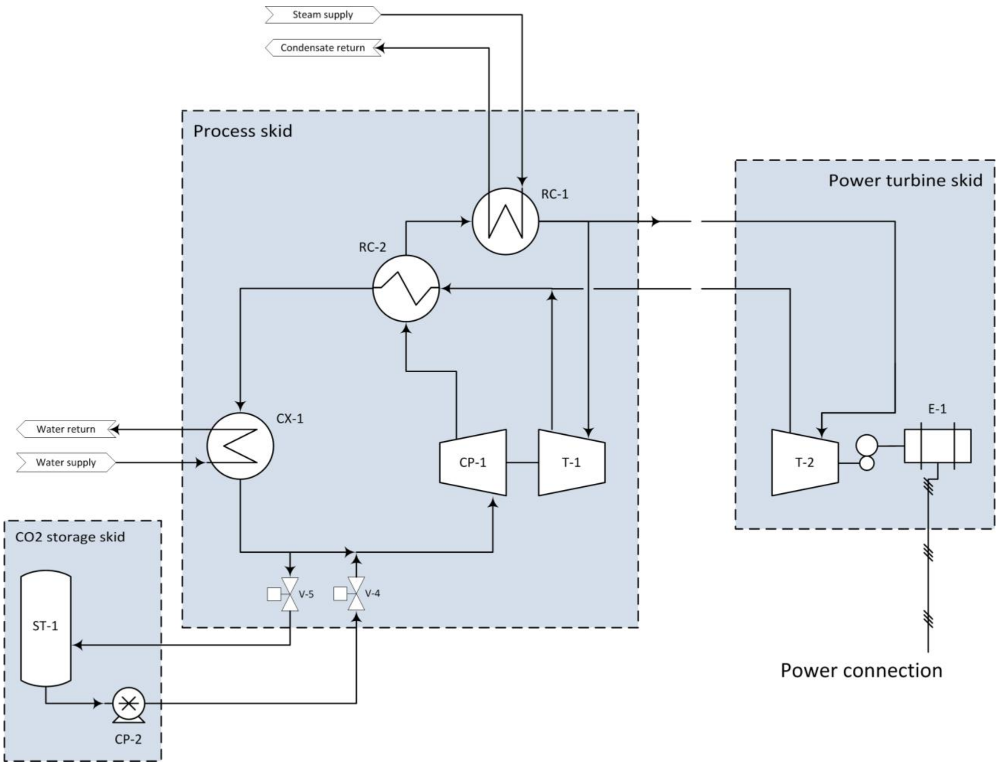

Figure 1: EPS100 test installation process flow diagram (PFD).

To properly evaluate the transient thermal stresses that PCHEs will be expected to withstand, it is first necessary to establish realistic transient boundary conditions that will be encountered in service. The present paper represents part of a larger study to define and validate a large-scale transient model of the EPS100 [10]. The full system model is still under development, and is not yet capable of simulating the entire operational envelope. Thus, for the present work, the sub-system model of the heat exchangers is used with imposed boundary conditions (inlet flows, temperatures and pressures) from the measured test data. This data set covers a broad range of operating conditions, which encompass system initial start, turbocompressor "bootstrapping," power turbine start, quasi-steady-state operation, and system trips. The transient performance of the heat exchanger model is compared to the measured responses of the two PCHEs in the EPS100 for model validation purposes. It is the intent of this study to establish the framework for full system simulations of extreme upset conditions, which can then be used to determine the expected cyclic life of the PCHEs.

MODELING PLATFORM

The transient simulations are conducted using the GT-SUITE [11] system simulation software platform. GT-SUITE is a 1D engineering system simulation software, and includes tools for analyzing mechanical, flow, thermal, electromagnetic and control systems. GT-SUITE solves 1D Navier-Stokes equations along flow components, and solution convergence is checked using pressure, continuity and energy residuals. Component models can be built based on GT-SUITE supplied and/or user-defined component templates. Component templates can utilize manufacturer data and/or test data to calibrate the component. Individual components, such as heat exchangers, pumps, turbines, can then be simulated and validated using subsystem boundary conditions. GT-SUITE uses NIST REFPROP [12] for calculating fluid thermal and transport properties. Further details of the modeling process and assumptions used in the overall system modeling can be found in Reference [10].

SYSTEM CONFIGURATION

The EPS100 is a 7.3MWe net power sCO_2 power cycle designed for commercial operation, utilizing the exhaust heat of a 20-25MWe gas turbine as the heat source. The details of the production cycle configuration and of an uprated version capable of over 9MWe from the same heat source, are described in Reference [3], and a simplified PFD in the as-tested configuration is shown in Figure 1. The EPS100 uses a constant-speed "power" turbine (T-2) connected to a gearbox-driven synchronous generator for power generation, and a separate, variable-speed turbocompressor (CP-1 and T-1) to provide high-pressure CO_2 to operate the cycle. In the as-tested configuration [7], the primary heat exchanger (RC-1) transfers heat from an external source (in this case, steam from facility boilers) to the working fluid, which then drives the two turbines in parallel. A single PCHE recuperator (RC-2) recovers residual enthalpy from the turbine exhausts by preheating the working fluid, and the remainder of the excess enthalpy is transferred to cooling tower water in the HRHX (CX-1), another PCHE.

HEAT EXCHANGER MODELS

In the present study, the recuperator and HRHX are simulated using the built-in plate heat exchanger (PHE) models in GT-SUITE. From a heat transfer and pressure loss perspective, PCHEs and PHEs have similar governing equations, as both are primarily counter-flow geometry, and the fluid flow is well within the turbulent regime. Thus, classical Nusselt number and friction factor functional forms of the heat transfer and pressure loss coefficients can be applied. The PCHE is simulated by applying a heat transfer area multiplier to account for the smaller passage dimensions relative to a conventional PHE. The heat transfer process is discretized into 25 sub-volumes to account for the variation in fluid properties as the temperature and pressure vary across the length of the heat exchanger. The thermal mass of the heat exchanger is set equal to the physical mass of the actual heat exchanger multiplied by the temperature-dependent heat capacity of the 316L stainless steel material. The heat transfer process is modeled as a series of thermal resistances. The baseline heat transfer coefficients are modeled after classical heat transfer correlations with variable coefficients, with a simple one-dimensional thermal conduction resistance between the two fluids.

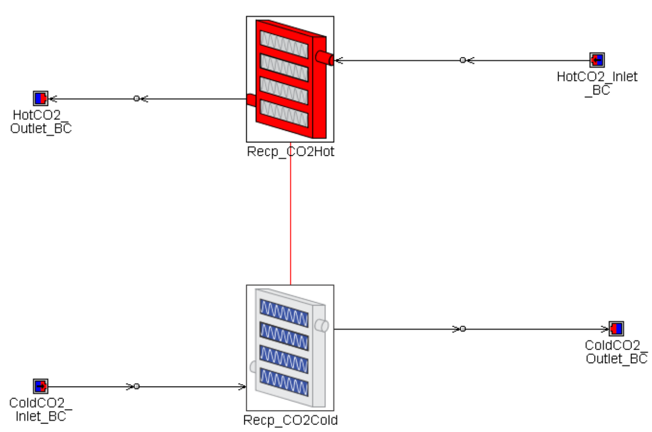

Figure 2: Recuperator model with boundary conditions

Figure 2 shows the recuperator model in isolation. Within the recuperator, relatively low-pressure, high-temperature CO_2 from the turbine exhaust transfers heat to the high-pressure, low-temperature CO_2 from the compressor discharge. The recuperator heat transfer coefficients are based on single-phase Dittus-Boelter correlations on both fluid sides, with coefficients calibrated using a subset of steady-state data points taken from test data. The calibration process utilizes measured fluid flow rates, inlet temperatures, inlet

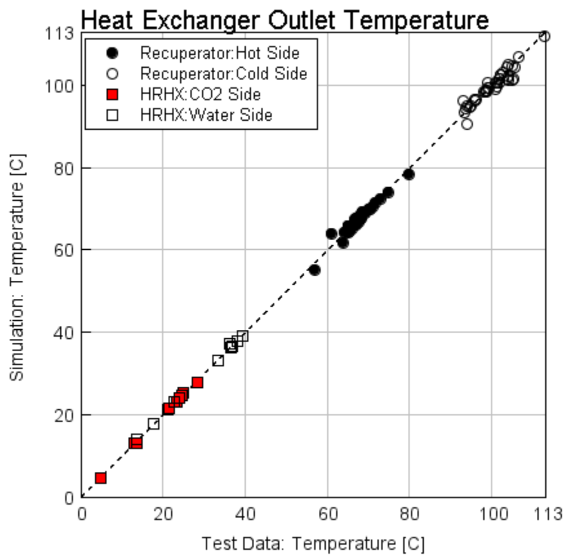

Figure 3: Recuperator and HRHX outlet temperatures from validation simulation

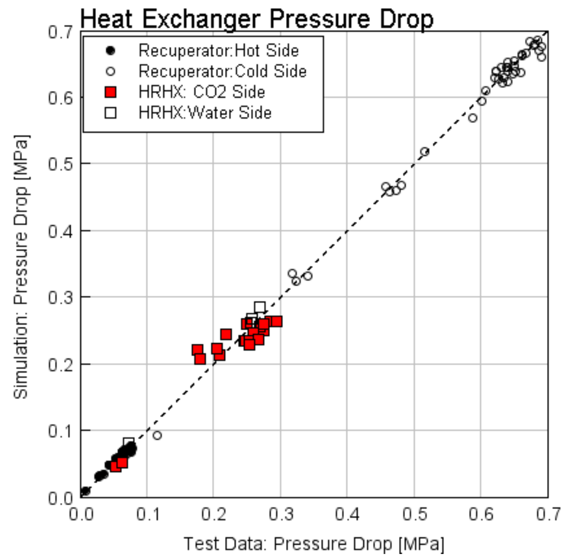

Figure 4: Recuperator and HRHX pressure drops from validation simulation

and outlet pressures, and overall heat transfer rate. Using this information, the software adjusts the heat transfer and pressure drop coefficients to best match the supplied data.

The PCHE water-cooled heat rejection heat exchanger model is constructed and validated in a similar manner as the recuperator. In the HRHX, CO_2 from the recuperator exhaust transfers heat to water from a cooling tower. As the EPS100 operates in both supercritical and transcritical (condensing) mode, the HRHX is modeled as a two-phase heat exchanger on the CO_2 side. For single-phase heat transfer, Dittus-Boelter correlations are used, while the correlation of Yan et al. [13] was used for condensation heat transfer.

The heat exchanger calibration process was validated by using simulating several steady-state operating points for the two heat exchangers. The modeled outlet conditions are shown in Figures 3 and 4 as a function of the measured outlet conditions. The agreement is excellent, with calculated weighted regression errors of 0.56% and 0.91% for overall heat transfer rate for the recuperator and HRHX respectively.

HEAT EXCHANGER SIMULATION RESULTS

The transient simulations are based on data collected during an extensive series of factory tests on the EPS100 system to evaluate operation, controls and performance [4]. Each day, the test system was run from a cold start to full load operation, with the goal of maximizing the power turbine output. For these simulations, the boundary condition values (heat exchanger inlet temperatures and flows) are taken from the test data, and input to the model, thus allowing the heat exchangers to be effectively modeled in isolation.

The overall comparison of the heat transfer rates and pressure drops across the recuperator and HRHX are shown in Figures 5-9. At the initial stage of the test, CO_2 is being circulated at a low rate through the system by a small motor-driven compressor, and heated by the primary heat exchanger. This flow causes the compressor drive turbine (T-1) to rotate at a relatively low speed, and the main compressor (CP-1) flow is diverted to the HRHX inlet through a bypass valve. Once the system is in an appropriate state (1591 seconds), the system operator commands the turbocompressor to transition to self-sustaining operation, termed “bootstrap,” and the main compressor flow supplies the drive turbine, which in turn causes it to accelerate to its nominal speed. Next, the power turbine (T-2), which was initially bypassed and isolated from the CO_2 flow rate, is accelerated to synchronous speed (“power turbine start”, 3986-4611 seconds), and then progressively loaded by connecting variable resistive load banks to the generator. The test was terminated by an indicated fault in one of the load banks at 31917 seconds, which resulted in a commanded system trip.

For the most part, the comparison is favorable, as would be expected following the calibration process as described previously. The time scale in these figures is too long to discern transient heat transfer effects, which are evaluated below.

One area in which the quasi-steady-state comparison is not acceptable is the CO_2-side pressure drop in the HRHX (note that while water-side pressure drop was measured, the inlet pressure transducer was upstream of the main water filter—thus, the data was unfortunately not usable for evaluation of the heat exchanger water-side pressure drop prediction). In Figure 9, the modeled CO_2-side pressure drop is seen to be in fair agreement after 10,000 seconds. At earlier times, the magnitude is generally correct, but the variation in pressure drop with time does not reflect the measurements. In addition, the modeled step change in pressure drop at 10,000 seconds does not appear to be physically realistic, and is not observed in the test data.

Upon closer examination, it appears that the key event associated with the change in behavior at 10,000 seconds is the transition of the HRHX inlet pressure from subcritical to supercritical at that time (Figure 10). As part of the system control strategy, the “low-side” pressure is actively controlled as a function of the measured compressor inlet temperature. Initially, the cooling tower water is relatively cold, both due to the thermal inertia of the water contained within the tower basin, and to the lower wet-bulb temperature in the early part of the day. As the test (and day) progressed, the cooling tower water temperature increased. The control system then increased the compressor inlet pressure in response to the higher measured CO_2 temperature at the compressor inlet. This caused the compressor inlet pressure to transition from subcritical to supercritical values.

During that time, the CO_2 flow within the HRHX is in the two-phase condensing regime—the numerical code automatically switches between single-phase and two-phase correlations. Therefore, it appears that the cause for the discrepancy lies within the two-phase pressure drop correlation or code execution. Initial efforts to understand the cause for the difference included evaluating alternate pressure drop correlations during the two-phase flow process, but without success. At this point, the root cause for the difference between the measured and modeled pressure drop is unknown. Interestingly although the recuperator inlet pressure transitioned from subcritical to supercritical, a similar discrepancy did not arise. However, since the subcritical operation of the recuperator takes place entirely within the vapor phase, the pressure drop correlation in use is still a single-phase formulation.

To evaluate the model’s capability of simulating the transient response of the recuperator and HRHX, the rapid thermal transients that occurred during the bootstrap process were examined in more detail. During steady-state operation, the amount of heat transferred from the hot fluid would be expected to equal the amount transferred to the cold fluid (with a small deviation due to external heat losses from the heat exchanger exterior surface to the environment). However, under transient heating conditions such as encountered during the bootstrap process, the thermal inertia of the heat exchanger should result in time delays between the hot-side heat transfer rate, and the cold-side heat transfer rate. This behavior can be observed in Figures 11 and 13 for both the recuperator and HRHX—the oscillations in heat transfer rate were due to corresponding oscillations in turbocompressor speed following the rapid acceleration to idle speed. Note that a simple characteristic time analysis yields estimated thermal response times of the order of 30-60 seconds, consistent with the measured thermal lag.

While the model accurately reproduces the hot fluid transient heat transfer rate, the initial modeling attempts greatly underestimated the thermal lag between the hot fluid and cold fluid response times. A parametric study of the input thermal mass of the heat exchanger (mass multiplied by heat capacity) was then conducted to estimate the magnitude of the discrepancy that the model. It was found that the thermal mass of the heat exchanger needed to be increased by an order of magnitude or more to achieve modeled thermal lag times comparable to the measured values (Figures 12 and 14). Further efforts are underway to establish the root cause for this discrepancy.

CONCLUSION

Initial transient modeling of the recuperator and HRHX heat exchangers in a 7.3MWe sCO_2 power cycle has been conducted. The quasi-steady-state heat transfer behavior of the heat exchangers, and the single-phase pressure drop behavior, can be modeled with reasonable accuracy. The pressure drop model does not accurately reproduce the measured data in the two-phase regime. The measured thermal lag behavior of both heat exchangers is in reasonable agreement with simplified characteristic time analysis. The baseline model greatly under-predicts the measured thermal lag behavior, and requires unrealistic modifications to the thermal mass of the heat exchangers to bring the model into agreement. The root cause of both these discrepancies is underway, and will be reported when available.

REFERENCES

[1] Le Pierres, R., Southall, D., and Osborne, S., 2011, "Impact of Mechanical Design Issues on Printed Circuit Heat Exchangers," *Proceedings of sCO_2 Power Cycle Symposium*, Boulder, Colorado.

[2] Dostal, V., Driscoll, M. J., and Hejzlar, P., 2004, *A Supercritical Carbon Dioxide Cycle for next Generation Nuclear Reactors*, Technical Report MIT-ANP-TR-100, Massachusetts Institute of Technology.

[3] Held, T. J., 2015, "Supercritical CO_2 Cycles for Gas Turbine Combined Cycle Power Plants," *Power Gen International*, Las Vegas, Nevada.

[4] Wright, S. A., Radel, R. F., Vernon, M. E., Rochau, G. E., and Pickard, P. S., 2010, *Operation and Analysis of a Supercritical CO_2 Brayton Cycle*, SAND2010-0171.

[5] Kimball, K. J., and Clementoni, E. M., 2014, "Supercritical Carbon Dioxide Brayton Power Cycle Development Overview," *The 4th International Symposium – Supercritical CO_2 Power Cycles*, Pittsburgh, Pennsylvania.

[6] Cho, J., Shin, H., Ra, H.-S., Lee, G., Roh, C., Lee, B., and Baik, Y.-J., 2016, "Development of the Supercritical Carbon Dioxide Power Cycle Experimental Loop in KIER," GT2016-57460, *ASME Turbo Expo 2016: Turbomachinery Technical Conference and Exposition*.

[7] Held, T. J., 2014, "Initial Test Results of a Megawatt-Class Supercritical CO2 Heat Engine," 4th Int.

Symp. - Supercrit. CO2 Power Cycles.

[8] Gezelius, K., 2004, “Design of Compact Intermediate Heat Exchangers for Gas Cooled Fast Reactors,” Massachusetts Institute of Technology.

[9] Pra, F., Tochon, P., Mauget, C., Fokkens, J., and Willemsen, S., 2008, “Promising Designs of Compact Heat Exchangers for Modular HTRs Using the Brayton Cycle,” Nucl. Eng. Des., **238**(11), pp. 3160–3173.

[10] Avadhanula, V. K., and Held, T. J., 2017, “Transient Modeling of a Supercritical CO_2 Power Cycle and Comparison with Test Data,” GT2017-63279, *ASME Turbo Expo 2017: Turbomachinery Technical Conference and Exposition*, Charlotte, NC.

[11] Anonymous, 2016, “GT-SUITE Overview” [Online]. Available: https://www.gtisoft.com/gt-suite/gt-suite-overview/. [Accessed: 21-Nov-2016].

[12] Lemmon, E. W., Huber, M. L., and McLinden, M. O., 2013, “NIST Standard Reference Database 23: Reference Fluid Thermodynamic and Transport properties—REFPROP.”

[13] Yan, Y.-Y., Lio, H.-C., and Lin, T.-F., 1999, “Condensation Heat Transfer and Pressure Drop of Refrigerant R-134a in a Plate Heat Exchanger,” Int. J. Heat Mass Transf., **42**(6), pp. 993–1006.

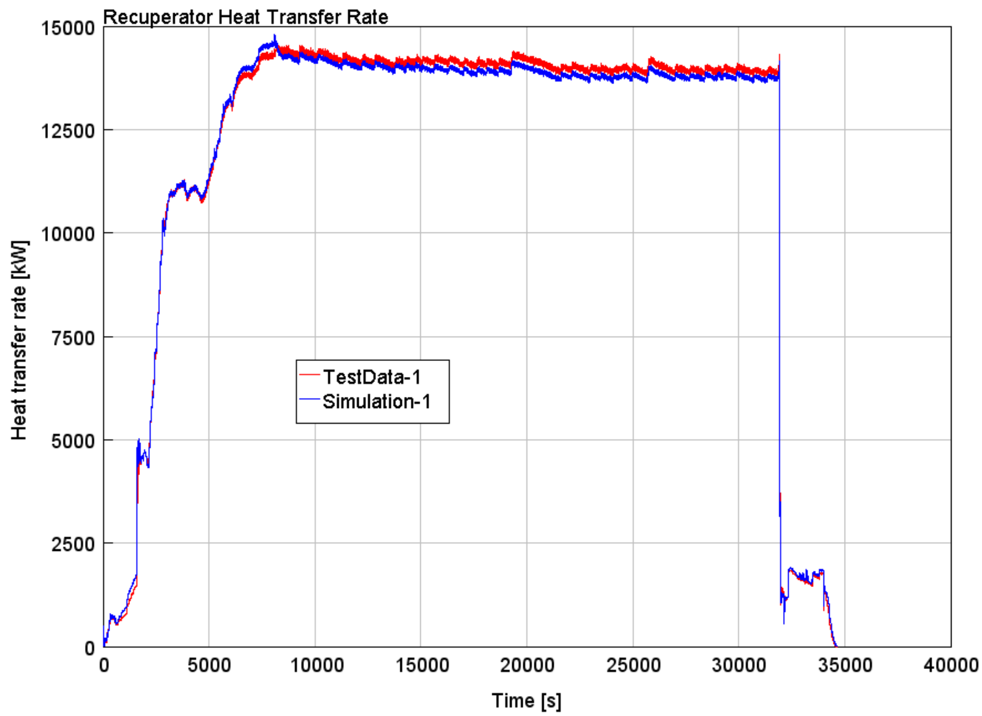

Figure 5: Recuperator heat transfer rate

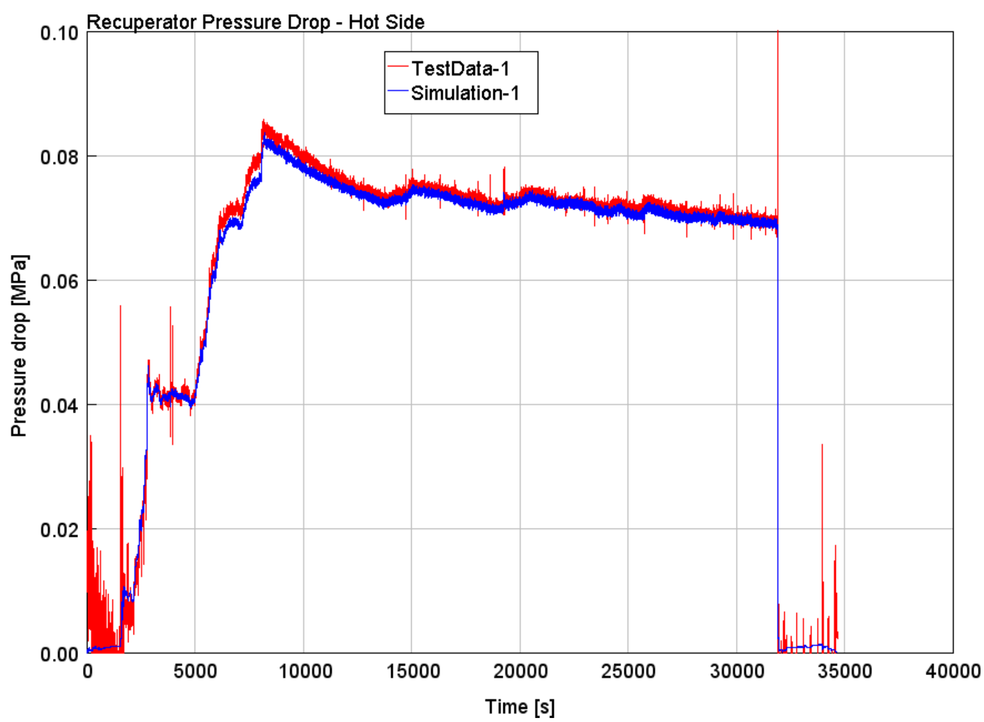

Figure 6: Recuperator low-pressure side pressure drop

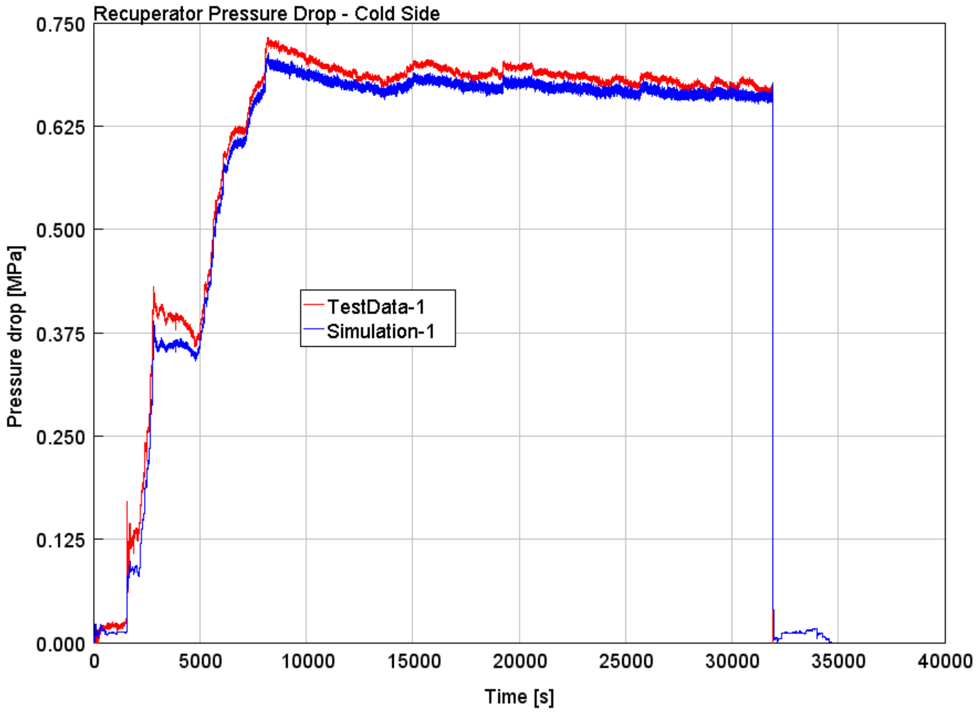

Figure 7: Recuperator high-pressure side pressure drop

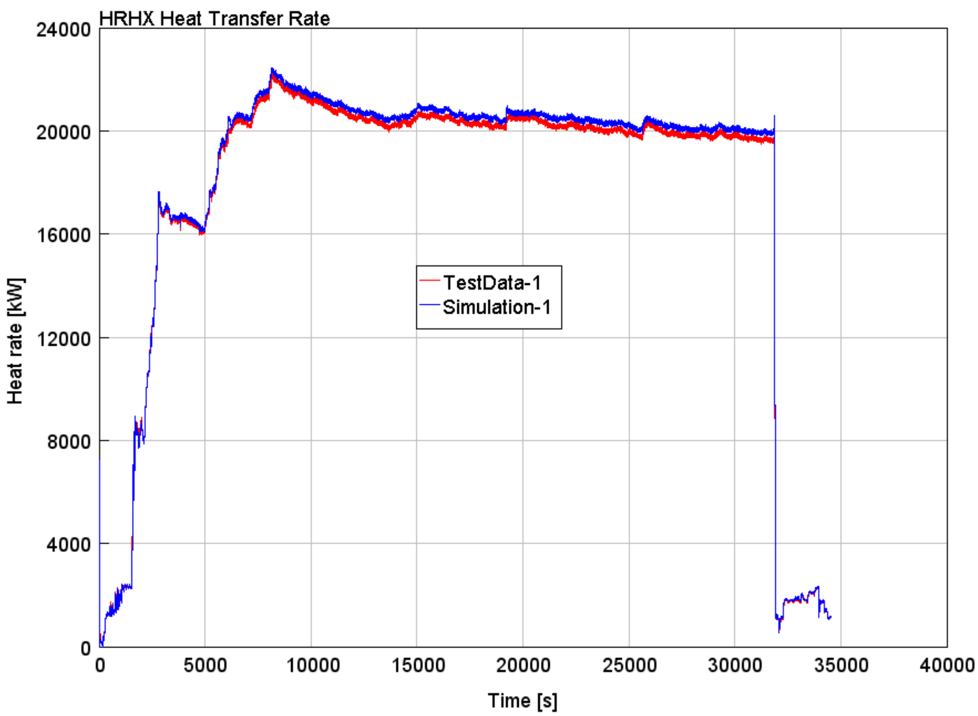

Figure 8: HRHX heat transfer rate

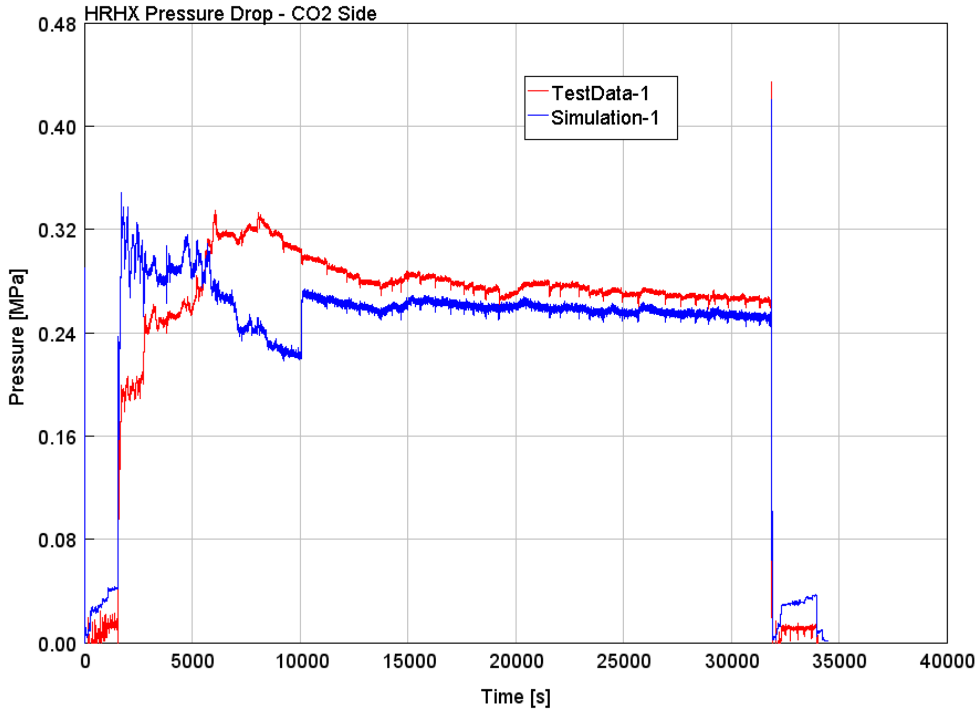

Figure 9: HRHX pressure drop on CO_2 side

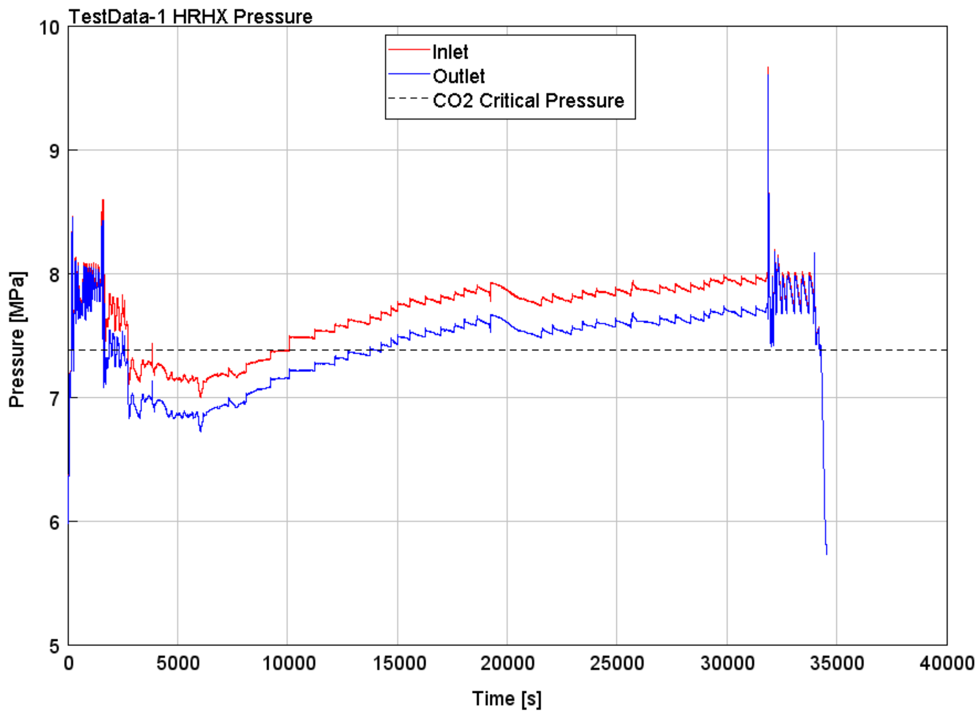

Figure 10: HRHX measured inlet and outlet pressures

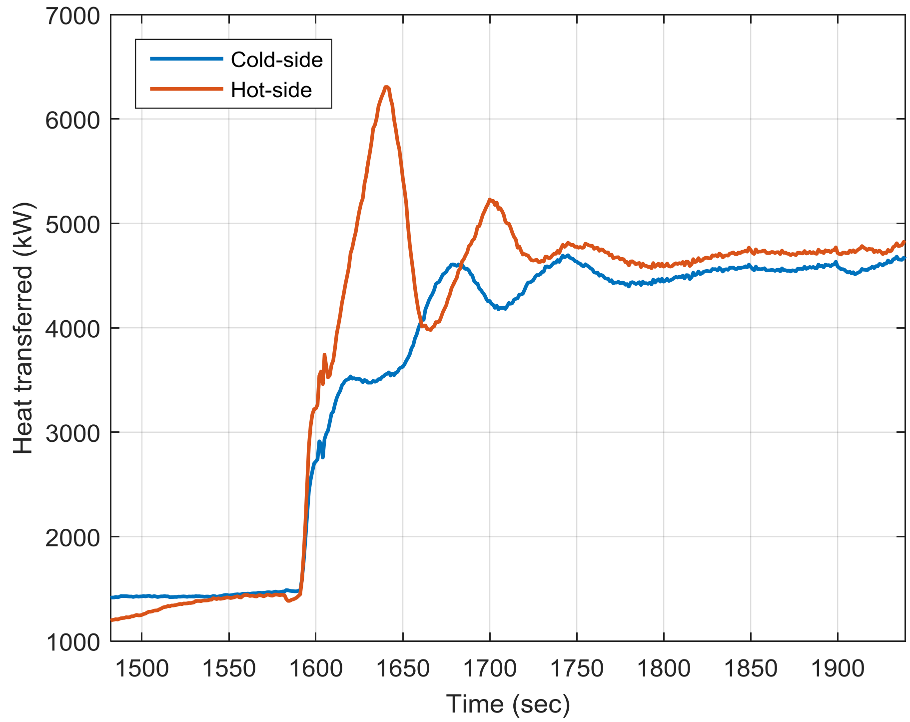

Figure 11: Measured thermal response of recuperator during rapid transient

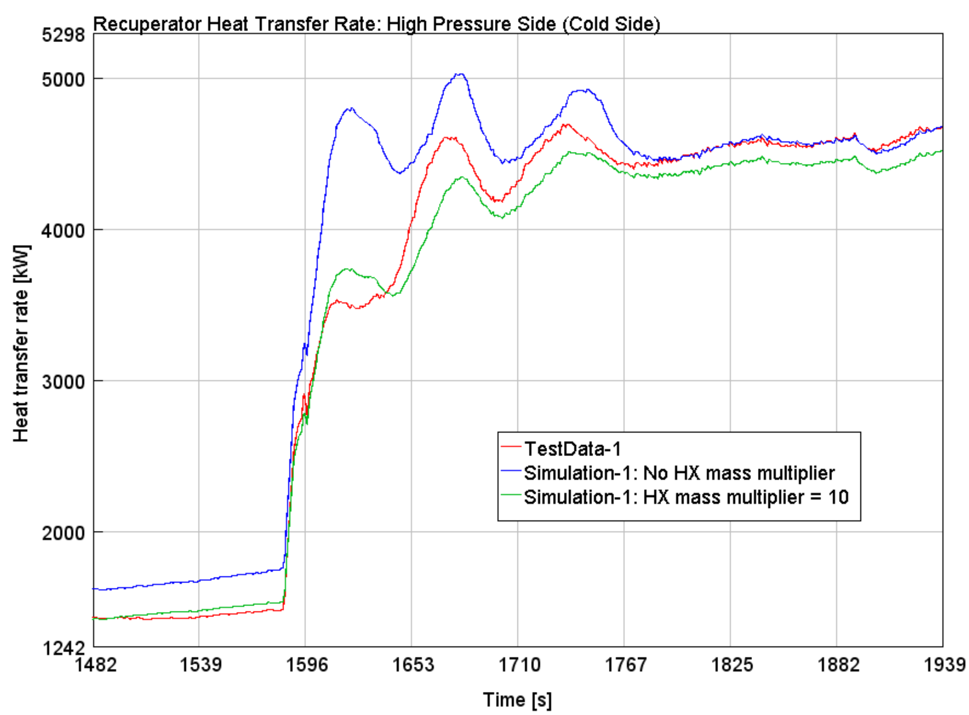

Figure 12: Modeled thermal response of recuperator during rapid transient with parametric variation of thermal mass

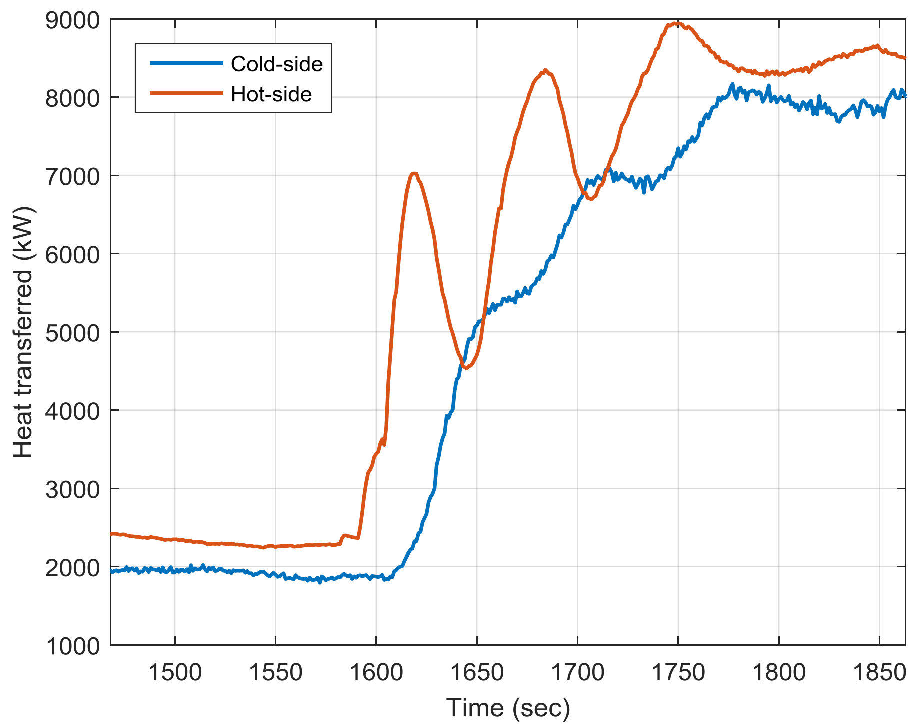

Figure 13: Measured thermal response of HRHX during rapid transient

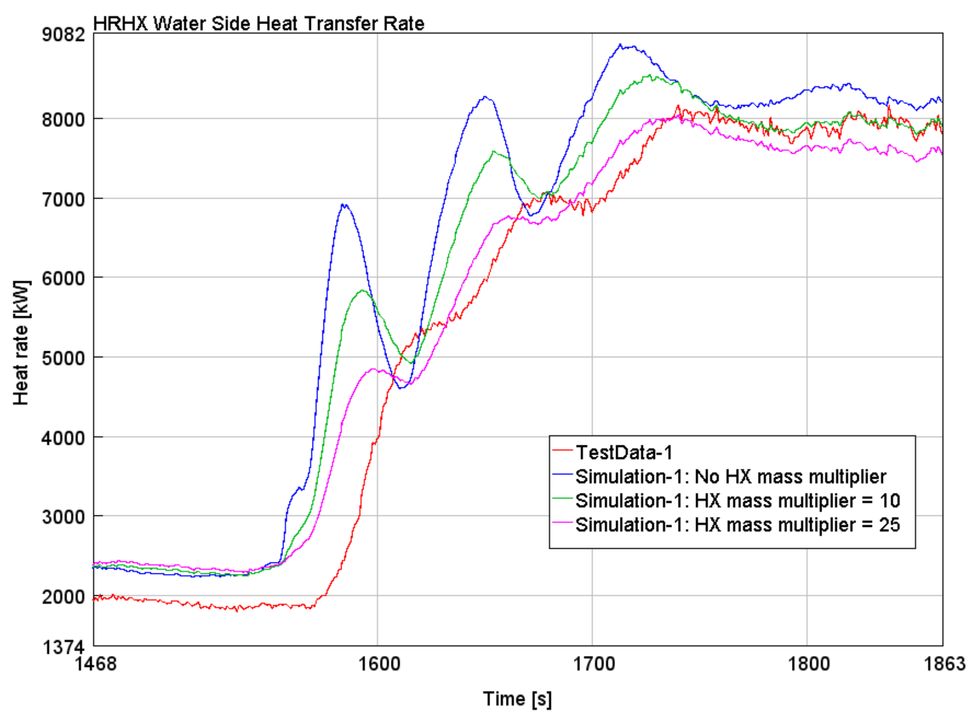

Figure 14: Modeled thermal response of HRHX during rapid transient